

Charge-state measurements of collectively accelerated heavy ions

W. W. Destler and J. T. Cremer
University of Maryland, College Park, Maryland 20742

(Received 26 August 1982; accepted for publication 26 October 1982)

Thomson spectrometer measurements of the charge states of collectively accelerated light and heavy ions (H, D, He, N, Ne, Ar) are reported. Within experimental error, all charge states are accelerated to the same peak energy for each ion specie. Relative ion flux densities for these ion species are also presented.

PACS numbers: 52.70.Nc, 52.60.+h, 52.75.Di, 52.80.Vp

I. INTRODUCTION

Linear-beam collective ion acceleration, where the intense space charge fields of an intense relativistic electron beam are used to accelerate ions, has been studied theoretically and experimentally at several laboratories¹⁻¹⁵ during the past decade. These studies have been centered around two different experimental configurations; one in which a linear electron beam is injected through a foil anode into a gas-filled drift tube, and another in which an ion source is provided at or near the anode plane. In the latter case, the ion sources have included dielectric anodes (the "Luce diode" configuration³), localized gas clouds,⁶ laser-plasma sources,⁷ discharge ion sources,⁸ and electron bombardment of conducting anodes and anode foils.⁹

Recently, experiments were reported by our group at the University of Maryland in which a fast-rise gas puff valve was used to provide a localized gas cloud downstream of the anode.^{10,11} The injected electron beam (1.5 MeV, 30 kA, 30 ns) ionized the gas and accelerated gas ions of various species (H, D, He, N, Ar, Kr, Xe) to very high energies. Using three different ion energy diagnostics, it was found that the peak velocity of the accelerated ions was approximately 0.1c, independent of the ion mass. This represents a peak ion energy of about 4.7 MeV/amu in all cases, corresponding to a peak Xe ion energy near 1 GeV. It was also determined that, for D, He, N, Ne, Ar, and Kr, the total ion charge collected by a

downstream charge collection probe was approximately constant.

In this paper, we present the results of experimental measurements of the charge states of these collectively accelerated heavy ions. In addition, we present measurements of the accelerated ion particle flux densities from these ion species which, together with the charge-state measurements, are consistent with the previous measurements of the total ion charge reported previously.¹¹ The experimental results are presented in Sec. II, and conclusions are drawn in Sec. III.

II. EXPERIMENTS

The experimental configuration used is shown in Fig. 1. An intense relativistic electron beam pulse (1 MeV, 30 kA, 30 ns) is field emitted from a 4-mm-diam cold tungsten cathode. The anode, a 6-mm thick stainless steel plate, has a 20-mm-diam hole on axis through which the beam passes into the downstream drift region. The diameter of the downstream drift tube is 15 cm. Ions to be accelerated are provided by electron beam ionization (and subsequent ion-ion avalanche ionization) of a neutral gas cloud from a fast puff valve. The timing of the puff valve firing and the positioning of the output nozzle of the puff valve are set such that the neutral gas cloud is located within 2 cm of the anode plane at

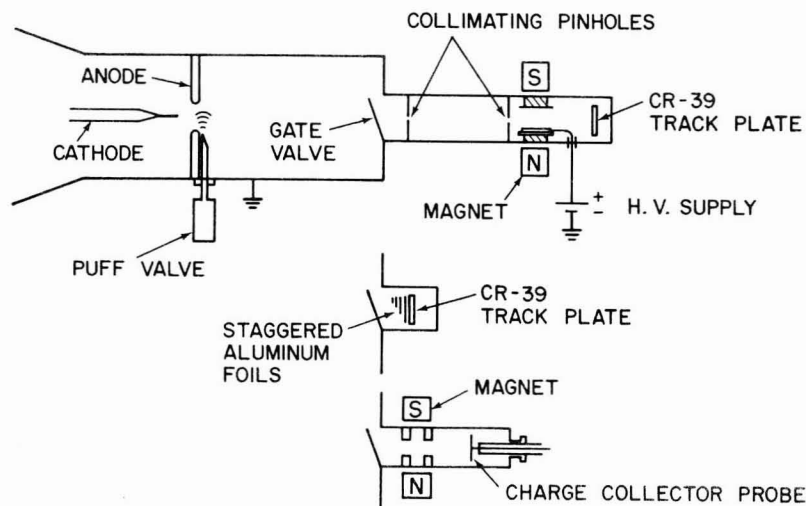


FIG. 1. General experimental configuration.

the time of electron beam injection. The ambient pressure in the diode and in the downstream tube is less than 1×10^{-4} Torr.

A. Charge-state measurements

Accelerated ion charge states were measured using a Thomson $E \parallel B$ spectrometer similar to that designed by M. J. Rhee.¹⁶ The ion beam is first collimated by two 0.2-mm pinholes separated by 23 cm. A magnetic field transverse to the collimated ion beam is provided by a permanent magnet and two pole pieces located inside the drift chamber. An insulated conducting plate located on the inside surface of one pole piece is connected to a high voltage power supply to provide an electric field parallel to the magnetic field. Typical values for E and B are 6×10^5 V/m and 0.2 T, respectively. Ions deflected by these fields are detected using a CR-39 track plate located 7 cm downstream of the pole pieces. The ion tracks become visible under a microscope after the exposed plate is etched in a NaOH solution.

Ions of a given charge to mass ratio Z/A and varying energy trace out a parabola on the track plate given theoretically by

$$x = 5.2 \times 10^{-9} \frac{E_x ((L_1^E)^2 + 2L_1^E L_2^E) y^2}{Z/A \left[\int_0^{L_1^E} \int_0^{L_2^E} B_x(z) dz dz \right]^2} \quad (\text{meters}), \quad (1)$$

where x is a coordinate in the direction of E and B (and therefore in the direction of electric field deflection) and y is the direction of magnetic field deflection. L_1^E is the distance over which the electric field is applied. In the absence of an accurate electric field measurement, E_x is assumed to be uniform over the distance L_1^E (the pole piece axial length) and zero outside the region of the pole pieces. L_2^E is the post-electric-field drift distance to the track plate, and L_1^B is the distance over which the magnetic field is applied (in this case the track plate is located at a position where the magnetic field is nonzero, so $L_2^B = 0$). For the particular experimental parameters used, this result reduces to

$$x = \frac{y^2}{20(Z/A)}, \quad (2)$$

where x and y are in millimeters.

Figure 2 shows the theoretical parabolas for helium ions (He^{+1} , He^{+2}) and a tracing of an electron microscope photograph of an actual experimentally obtained track plate. Figure 3 shows comparable results for nitrogen ions. The coordinate axes and the coordinate origin may be obtained easily by simply setting either E_x or B_x to zero, or both, and accelerating ions in the normal fashion. For the lighter ions, only one shot is necessary to produce the desired parabolas or axes. For the heavier ions, however, the number of ions accelerated per shot is significantly less (as will be discussed in the next section), and several shots are required to obtain reasonable results.

It is easily shown that, in theory, any straight line drawn from the origin in the x - y plane is a constant velocity contour. That is, ions that are observed on this line will all have the same velocity. From the data shown in Fig. 2, it is seen that He^{+1} and He^{+2} are both accelerated to approxi-

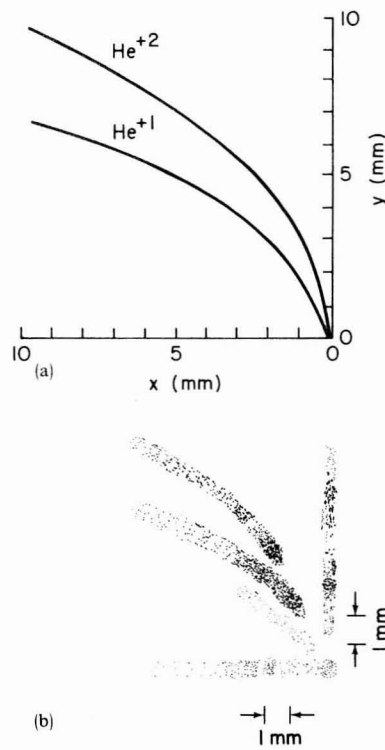


FIG. 2. (a) Theoretical parabolas for He^{+1} and He^{+2} . (b) Electron microscope photograph of CR-39 track plate showing He^{+1} and He^{+2} parabolas.

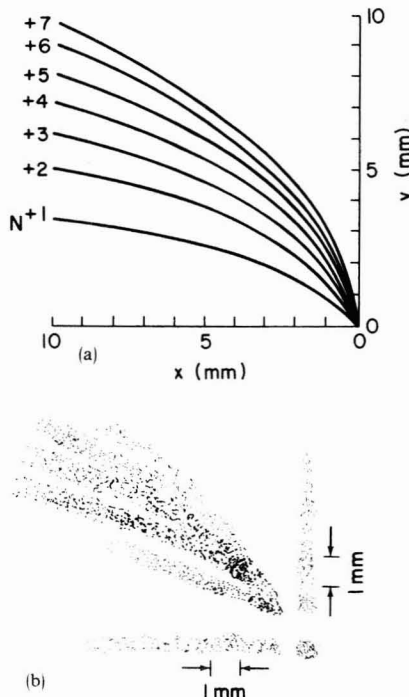


FIG. 3. (a) Theoretical parabolas for N^{+1} - N^{+7} . (b) Experimentally obtained parabolas for nitrogen.

TABLE I. Results of Thomson spectrometer measurement of ion charge states.

Injected gas	Highest Z/A	Lowest Z/A	Notes
H	1	1/2	H_2^+ (?)
D	1/2	1/4	D_2^+ (?)
He	1/2	1/4	Low Z/A impurity ions
N	5/14	1/14	
Ne	7/20	1/20	
Ar	$\sim 14/40$	$\sim 1/40$	

mately the same peak velocity (and therefore peak energy). This observation holds for the other ion species investigated as well.

The results of these studies are summarized in Table I. A number of additional remarks should be made at this point: (1) As the mass of the accelerated ion specie increases, so does the number of possible charge states. The resolution of the spectrometer is not good enough to resolve individual charge states for ions heavier than neon. Thus, the results for argon are approximate. (2) No attempt was made to accelerate ions to the highest possible energy. Peak energies observed in these experiments (performed at 1 MeV electron beam energy versus 1.5 MeV for the previous work¹¹) were about 1 MeV/amu. Thomson spectrometry is not a very good diagnostic for determining peak ion energy, since resolution is poorest at high ion energy. (3) There is no evidence of significant proton acceleration when gases other than hydrogen were used. (4) As expected, the individual ion-track etch pits in the CR-39 plate increased in diameter as the mass of the accelerated ion was increased. (5) The total number of ion tracks is fairly evenly distributed among the observed charge states, with the highest charge state, as expected, having the lowest population level. (6) The presence of parabolas with indicated values of Z/A of 1/2 for hydrogen and 1/4 for deuterium is most likely attributable to the presence of H_2^+ and D_2^+ . Molecular hydrogen and deuterium ions are routinely observed in other ion sources. (7) The low Z/A impurity ions noted in the helium shots are not always observed, and may be attributable to iron ions drawn off of the anode by the electron beam. The resolution of the spectrometer is not sufficient to positively identify these impurities.

B. Ion particle flux measurements

Information on the number of ions accelerated to energies above about 3 MeV/amu have been obtained using the configuration shown in Fig. 1. In these experiments, the electron beam energy was about 1.5 MeV, and as reported previously,¹¹ the peak ion energy observed is about 5 MeV/amu for all ion species. In these experiments, the ions are passed through staggered 0.65-mil aluminum stopping foils onto a CR-39 track plate. If the energy necessary to produce a track is assumed small, a rough picture of the high-energy end of the ion energy spectrum can be obtained by counting the ion tracks per square centimeter from ions that pass through a known thickness of stopping foils. Such spectra are shown in Fig. 4 for He, Ne, and Xe ions. The spectra below about 2–3

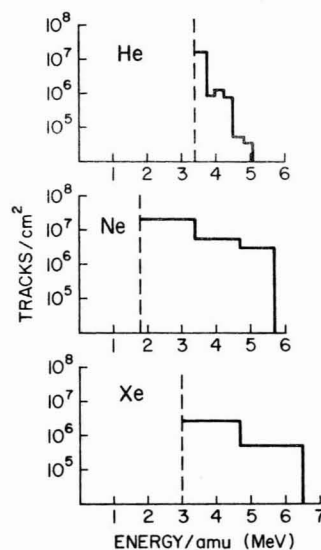


FIG. 4. Typical accelerated ion-energy spectra obtained from the staggered foil, range energy-track etching technique.

MeV/amu cannot be determined in this manner, because the tracks overlap at low energies, making counting impossible. These results indicate that the number of ions accelerated to energies in excess of about 3 MeV/amu decreases as the ion mass increases. This result is shown more clearly in Fig. 5, where the number of ions/per square centimeter accelerated to energies above 3 MeV/amu (obtained from the track counting technique) is plotted versus ion mass.

III. CONCLUSIONS

The results of these measurements shed important new light on the previously reported results. It is now clear that as the ion mass increases, the average charge per ion increases,

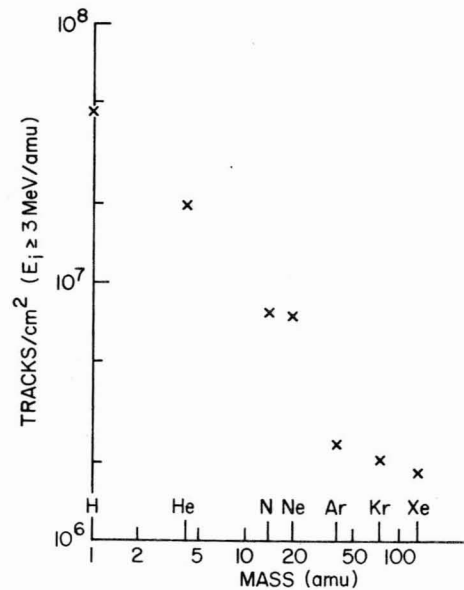


FIG. 5. Ion tracks/cm² plotted as a function of ion mass for ion energies greater than 3 MeV/amu.

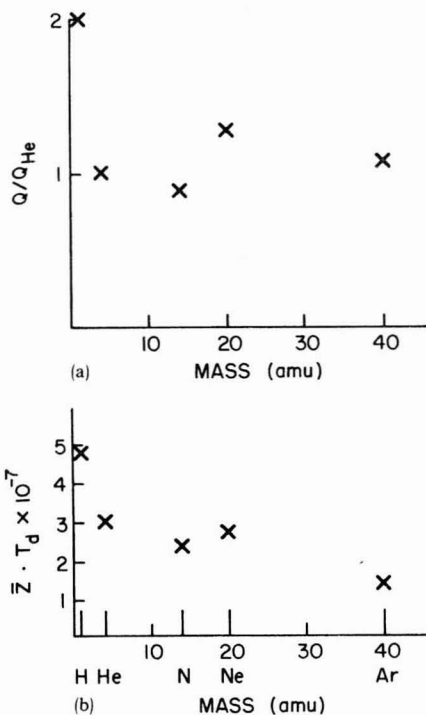


FIG. 6. (a) Total ion charge collected by a charge collection probe 55 cm downstream of the anode (normalized to that for helium) vs ion mass. (b) $\bar{Z} \cdot T_d$ plotted vs ion mass.

but the number of ions accelerated decreases. This result is shown graphically in Fig. 5(b). Here the product of the "average" ion charge state [$\bar{Z} = (Z_{\max} + Z_{\min})/2$] with the observed track density (cm^{-2}) (for ions with energies above 3 MeV/amu) T_d is plotted as a function of ion mass. These results may be compared with previously obtained measurements of the total ion charge collected by a charge collection probe placed in the downstream region immediately after an electron sweeping magnet (see Fig. 1). This total charge collected (normalized to that collected for helium) is plotted versus ion mass and shown in Fig. 6(a). From the similarity between Figs. 6(a) and 6(b), it is clear that although the total

charge collected is roughly constant for He, N, Ne, and Ar, this effect results from the combined trends of higher average charge per ion and lower particle number as the ion mass increases.

The observed fact that each charge state is accelerated to approximately the same velocity is a strong argument that the acceleration is not electrostatic, in which case the higher-charge-state ions should reach higher energies, but more likely the result of a moving potential well.

ACKNOWLEDGMENTS

It is a pleasure to acknowledge useful discussions with Professor M. Reiser, Professor M. J. Rhee, Professor C. D. Striffler, and Mr. L. E. Floyd. Assistance with the data analysis was provided by J. Gregor, and technical assistance was provided by D. N. Cohen and J. Pyle. This work was supported by the Air Force Office of Scientific Research and the U.S. Department of Energy.

¹C. L. Olson and U. Schumacher, in *Springer Tracts in Modern Physics: Collective Ion Acceleration*, edited by G. Hohler (Springer, New York, 1979), Vol. 84.

²S. Graybill and J. Uglum, *J. Appl. Phys.* **41**, 236 (1970).

³J. S. Luce, *Ann. N. Y. Acad. Sci.* **20**, 336 (1973).

⁴E. D. Korop and A. A. Plyutto, *Zh. Tekh. Fiz.* **41**, 1055 (1971) [*Sov. Phys. Tech. Phys.* **16**, 830 (1971)].

⁵A. A. Plyutto, *Sov. Phys. JETP* **12**, 1106 (1961).

⁶W. W. Destler, L. Floyd, and M. Reiser, *IEEE Trans. Nucl. Sci.* **26**, 4177 (1979).

⁷W. W. Destler, H. S. Uhm, H. Kim, and M. Reiser, *J. Appl. Phys.* **50**, 3015 (1979).

⁸J. A. Nation, G. Providakes, and V. Serlin, in *Proceedings of the Fourth International Topical Conference on High Power Electron and Ion Beam Research and Technology*, Palaiseau, France, 1981, p. 667.

⁹R. J. Adler and J. A. Nation, *Appl. Phys. Lett.* **36**, 310 (1980).

¹⁰W. W. Destler, L. E. Floyd, and M. Reiser, *Phys. Rev. Lett.* **44**, 70 (1980).

¹¹L. E. Floyd, W. W. Destler, M. Reiser, and H. M. Shin, *J. Appl. Phys.* **52**, 693 (1981).

¹²P. L. Taylor, *J. Appl. Phys.* **51**, 22 (1980).

¹³L. S. Bogdankevich, I. L. Zhelyazkov, and A. A. Rukhadze, *Sov. Phys. JETP* **30**, 174 (1970).

¹⁴M. Masuzaki, Y. Tamagawa, K. Kamada, S. Watanabe, S. Kawasaki, Y. Kubota, and T. Nakanishi, *Jpn. J. Appl. Phys.* **21**, L326 (1982).

¹⁵J. W. Poukey and N. Rostoker, *Plasma Phys.* **13**, 897 (1971).

¹⁶M. J. Rhee, *IEEE Trans. Nucl. Sci.* **28**, 2663 (1981).